https://doi.org/10.22226/2410-3535-2021-4-422-426 PACS: 46.50.+a

Prediction of the fatigue life of VT1-0 titanium in various structural states under very high cycle fatigue

D. R. Ledon[†,1,2], M. V. Bannikov[1], V. A. Oborin[1], Yu. V. Bayandin[1], O. B. Naimark[1]

[†]ledon@icmm.ru

[1]Institute of Continuous Media Mechanics UB RAS, Perm, 614013, Russia
[2]Ioffe Physical Technical Institute RAS, St. Petersburg, 194021, Russia

The paper presents an experimental methodology for assessing the ultra-high-cycle resource as applied to titanium VT1-0 in the submicrocrystalline and nanostructured states. The program for testing very-high-cycle loading (number of cycles 10^7–10^9) has been experimentally implemented. An "*in situ*" technique for determining the accumulation of irreversible fatigue damage was used. This technique is based on the analysis of nonlinear manifestations of the feedback signal in a closed system of an ultrasonic fatigue unit. This makes it possible to establish a connection between microscopic mechanisms of fatigue and model concepts and to consider the stages of damage development based on the nonlinear kinetics of defect accumulation during cyclic loading in the regimes of high- and very-high-cycle fatigue. A mathematical model of a deformable solid based on wide-range constitutive relations of the statistical theory of defects is presented. The proposed model contains a structural scaling parameter that allows one to describe the deformation behavior and fracture of the material under study in various structural states. The effect of damage accumulation under gigacycle loading is described. Numerical calculations predict well the experimental Wöhler curves. In an axisymmetric formulation, a boundary value problem is solved — the process of emergence of a crack originating inside the material is modeled.

Keywords: titanium VT1-0, fracture, very-high-cycle fatigue.

УДК: 539.388.1; 539.431; 539.422.24

Прогнозирование усталостной долговечности титана ВТ1-0 в различных структурных состояниях при сверхмногоцикловой усталости

Ледон Д. Р.[†,1,2], Банников М. В.[1], Оборин В. А.[1], Баяндин Ю. В.[1], Наймарк О. Б.[1]

[1]Институт механики сплошных сред УрО РАН, Пермь, 614013, Россия
[2]Физико-технический институт им. А. Ф. Иоффе РАН, Санкт-Петербург, 194021, Россия

В работе приведена экспериментальная методология оценки сверхмногоциклового ресурса применительно к титану ВТ1-0 в субмикрокристаллическом и наноструктурированном состояниях. Экспериментально реализована программа испытаний сверхмногоциклового нагружения (количество циклов 10^7–10^9) с применением методики «*in situ*» определения накопления необратимых усталостных повреждений, основанной на анализе нелинейных проявлений сигнала обратной связи в замкнутой системе ультразвуковой усталостной установки, которая позволяет установить связь микроскопических механизмов усталости с модельными представлениями, а также рассматривать стадийность развития поврежденности на основе нелинейной кинетики накопления дефектов в процессе циклического нагружения в режимах много- и гигацикловой усталости. Представлена математическая модель деформируемого твёрдого тела, базирующаяся на широкодиапазонных определяющих соотношениях статистической теории дефектов. Предложенная модель содержит параметр структурного скейлинга, позволяющий описывать деформационное поведение и разрушение исследуемого материала в различных структурных состояниях. Описан эффект накопления повреждённости при гигацикловом нагружении. Численные расчёты хорошо предсказывают экспериментальные кривые Вёлера. В осесимметричной постановке решена краевая задача — смоделирован процесс выхода на поверхность трещины, зародившейся внутри материала.

Ключевые слова: титан ВТ1-0, разрушение, гигацикловая усталость.

1. Introduction

Determination of the origin of fatigue cracks is one of the most important fundamental problems for various fields of application, especially when it comes to very-high-cycle (gigacycle) [1] fatigue (VHCF) with a crack origin inside the material. A characteristic feature of the development of fracture under gigacycle fatigue is the decisive influence on the fatigue life of the crack initiation stage. At the same time, the qualitative difference is the formation of a fatigue crack in the bulk of the material [1–2], which decisively changes the formulation of the problem of assessing the fatigue life, methods for studying the stages of development of fracture. In the field of high-cycle fatigue, the focus is on the crack propagation stage. Under gigacycle fatigue, a fundamental problem arises about crack initiation during multiscale damage development processes associated with defects of various nature (inclusions, localized plastic shear bands, microcracks, pores).

The formation of an ultrafine-grained structure by the methods of severe plastic deformation leads to a significant increase in the strength properties of metallic materials both in quasi-static [3–7] and cyclic tests [8–11]. Therefore, the study of the fatigue characteristics of titanium alloys with an ultrafine-grained structure is an urgent task. When studying the mechanisms of formation of fatigue cracks [1,11–12], it is noted that the staging of fracture is characterized by the effects of "irreversibility" related to localized shears. This aspect plays a key role in the initiation of a fatigue crack, with pronounced nonlinearity of the elastic behavior of materials. The technique of analysis of nonlinear vibrations [13–15] has been widely used for assessing the initiation and growth of fatigue cracks [16–20]. This technology allows *"in situ"* to assess the state of material damage during testing based on the manifestation of anomalies of elastic properties, measured by the amplitude of the second harmonic of the free end of the sample. Laboratory tests make it possible to substantiate the applicability of mathematical models capable of adequately describing fracture processes under fatigue loading.

2. Material and Experiment Conditions

Technical pure titanium VT1-0 was selected as the material under study in two states: submicrocrystalline (SMC) with a characteristic grain size of 193 nm and nanostructured (NS) with a characteristic grain size of 117 nm. These states are obtained by combining the methods of helical rolling with longitudinal section rolling and described in [21]. The structure of these materials is described and studied in [22–24]. This material is used for products with high strength, sufficient ductility and viscosity, high resistance to fatigue fracture. It is used in mechanical engineering, instrument making, instrumental industry, for the manufacture of products of cryogenic technology, as well as in medicine for the manufacture of implants.

The samples, which are cylinders with variable cross-section (Fig. 1), were subjected to cyclic tests (with the cycle asymmetry coefficient $R=-1$) on a Shimadzu USF-2000 resonant-type testing machine with a frequency of 20 kHz. During loading, the samples were subjected to abundant air cooling with compressed air. The stress amplitude was determined through displacements according to analytical formulas. The testing machine software performs the opposite procedure, allowing the voltage amplitude to be set, which is converted to the displacement amplitude.

SMC and NS states exhibit a scatter of properties (Fig. 2). For example, at practically identical stresses, the number of cycles to failure differs by orders of magnitude. Nevertheless, certain trends can be identified. The SMC state demonstrates a greater endurance limit in the VHCF region — 320 MPa based on $2\cdot10^9$ cycles, and the NS state on the same base shows 250 MPa.

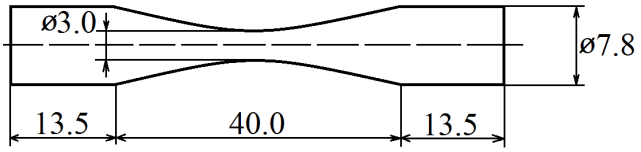

Fig. 1. Geometry of specimens for fatigue tests. Dimensions are in mm.

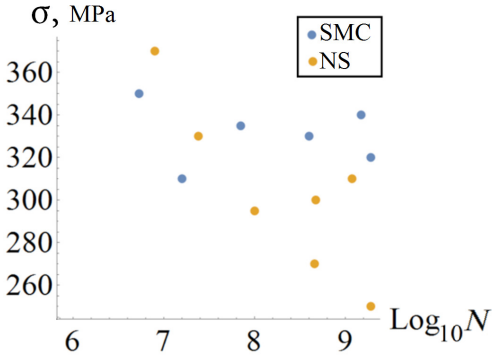

Fig. 2. (Color online) Results of fatigue tests for SMC and NS states.

3. Method for assessing material damage during fatigue tests by vibrations of the free end

Oscillations of the free end of the sample during testing will contain a number of harmonic components: components with amplitude A_1 at the fundamental frequency ω_0, amplitude A_2 of the second harmonic at frequency $2\omega_0$, and so on. Let us introduce the nonlinearity parameter β^e, which is determined experimentally by measuring the absolute amplitudes of the signals of the first A_1 and second A_2 harmonics corresponding to the nonlinear law of elasticity:

$$\sigma = A_2^e\left(\frac{\partial u}{\partial a}\right)+\left(\frac{1}{2}\right)A_3^e\left(\frac{\partial u}{\partial a}\right)^2+\ldots = A_2^e\left[\left(\frac{\partial u}{\partial a}\right)-\frac{1}{2}\beta^e\left(\frac{\partial u}{\partial a}\right)^2+\ldots\right],$$

where σ is the load, u is the displacement, a is the spatial coordinate, A_2^e and A_3^e are the elastic coefficients of the second and third order, respectively. Introducing the nonlinearity coefficient:

$$\beta^e = -A_3^e / A_2^e.$$

Then the wave equation can be represented as:

$$\frac{\partial^2 u}{\partial t^2} = c^2\left[1-\beta^e\left(\frac{\partial u}{\partial a}\right)\right]\left(\frac{\partial^2 u}{\partial a^2}\right),$$

where u is the component of the displacement vector in the a direction, c is the longitudinal speed of sound, and t is time.

Its solution, taking into account that the perturbation of the end,

$$u = u_1 \cos(\omega t),$$

will have the form:

$$u = u_0 + u_1 \cos(\omega t) + u_2 \sin(2(\omega t - ka)) + ...,$$

where

$$u_2 = \frac{1}{8k^2 \beta^e u_1^2 a},$$

$k = \omega_0/v$ — wave number. Then:

$$\beta^e = \frac{8u_2}{k^2 u_1^2 a}.$$

In the study of nonlinear phenomena in the gigacycle fatigue mode by measuring the amplitudes of the fundamental and second harmonics, the relative parameter is determined: $\beta_{relative} = \beta^e/\beta_0^e$, where β_0^e refers to undamaged material. To determine the nonlinearity coefficient, let us logarithm:

$$\log(\beta) = \log(k) + \log(u_2) - 2\log(u_1),$$

$$A_1 = 20\log(u_1), \quad A_2 = 20\log(u_2),$$

then:

$$20\log(\beta) = 20\log(k) + 20\log(u_2) - 40\log(u_1),$$

$$20\log(\beta) = K + A_2 - 2A_1.$$

Thus, the relative parameter of nonlinearity can be found from the formula:

$$20\log(\beta/\beta_0) = (A_2 - 2A_1) - (A_2 - 2A_1)_0.$$

The amplitude was measured with an inductive sensor with a signal recording frequency of 10 MHz. Time intervals of 65 536 points with a recording frequency of 100 kHz were analyzed.

Despite the fact that the process of fatigue crack formation is of a purely local nature, the formation of internal defects contributes to the integral characteristics of the material, such as Young's modulus. It is assumed that the sensitivity of the inductive displacement sensor makes it possible to capture such changes in the vibration amplitude. It can predict the onset of crack initiation and will make it possible to create new methods for monitoring and preventing fatigue failure. The change in the second harmonic amplitude in this work is associated with the presence of internal defects. An abrupt change signals a significant change in elastic modulus caused by a large defect such as a crack. The developed "feedback" system analyzed the average value of the second harmonic amplitude. If it began to increase sharply, it stopped testing and signaled the possible initiation of a fatigue crack. An example of measurement results is shown in Fig. 3. It can be seen that an avalanche-like increase in the second harmonic amplitude is observed at the moment preceding the failure.

4. Mathematical Modeling

The proposed mathematical model for describing fracture under fatigue loading, based on the wide-range constitutive relations of the statistical theory [25 – 26], has the following form:

$$\rho \dot{\mathbf{v}} = \nabla \cdot \boldsymbol{\sigma}, \tag{1}$$

$$\dot{\rho} + \rho \nabla \cdot \mathbf{v} = 0, \tag{2}$$

$$\mathbf{D} = \frac{1}{2}\left(\nabla \mathbf{v} + \nabla \mathbf{v}^T\right), \tag{3}$$

$$\boldsymbol{\sigma} = \boldsymbol{\sigma}_s + \boldsymbol{\sigma}_d, \quad \boldsymbol{\sigma}_s = \frac{1}{3}\boldsymbol{\sigma} : \mathbf{E}, \tag{4}$$

$$\boldsymbol{\sigma}^R = \lambda\left(\mathbf{D} : \mathbf{E}\right)\mathbf{E} + 2G(\mathbf{D} - \dot{\boldsymbol{\varepsilon}}^p - \dot{\mathbf{p}}), \tag{5}$$

$$\boldsymbol{\sigma}^R = \dot{\boldsymbol{\sigma}} - \dot{\mathbf{R}} \cdot \mathbf{R}^T \cdot \boldsymbol{\sigma} + \boldsymbol{\sigma} \cdot \dot{\mathbf{R}} \cdot \mathbf{R}^T, \tag{6}$$

$$\dot{\boldsymbol{\varepsilon}}^p = \dot{\varepsilon}_0^{n_\varepsilon} \exp\left(\frac{U(T)}{kT}\right)\left(\Gamma_\sigma \boldsymbol{\sigma} - \Gamma_{p\sigma} \frac{\partial F}{\partial \mathbf{p}}\right), \tag{7}$$

$$\dot{\mathbf{p}} = \dot{\varepsilon}_0^{n_p} \exp\left(\frac{U(T)}{kT}\right)\left(\Gamma_{p\sigma} \boldsymbol{\sigma} - \Gamma_p \frac{\partial F}{\partial \mathbf{p}}\right), \tag{8}$$

$$\dot{\delta} = -\dot{\varepsilon}_0^{n_\delta} \Gamma_\delta \frac{\partial F}{\partial \delta}, \tag{9}$$

$$U(T) = \frac{k}{T_c^m} T^{m+1}, \tag{10}$$

$$\frac{F}{F_m} = \frac{p^2}{2} - \frac{p^2}{2\delta} + c_1 p + c_2 \ln(c_3 + c_4 p + p^2) - \frac{\boldsymbol{\sigma}_d : \mathbf{p}}{2G}, \tag{11}$$

$$\rho c \dot{T} = \boldsymbol{\sigma} : \dot{\boldsymbol{\varepsilon}}^p - \frac{\partial F}{\partial \mathbf{p}} : \dot{\mathbf{p}} + \alpha \Delta \mathbf{T}, \tag{12}$$

where ρ is the mass density; $\mathbf{v}$ is the velocity vector; $\boldsymbol{\sigma}$ is the stress tensor, $\boldsymbol{\sigma}_s$ and $\boldsymbol{\sigma}_d$ are its spherical and deviatorial parts; $\nabla(\cdot)$ is the gradient operator in the current configuration; $\dot{(\cdot)}$ is the material derivative; $\mathbf{D}$ is the strain rate tensor, $\boldsymbol{\varepsilon}^p$ is the plastic strain tensor; λ and G are elastic constants of the material; $\mathbf{E}$ is the unit tensor; $\dot{\varepsilon}_0 = \sqrt{(2/3)\mathbf{D} : \mathbf{D}}/\dot{\varepsilon}_c$, $\dot{\varepsilon}_c = 1\ s^{-1}$ is the dimensionless multiplier; k is the Boltzmann constant; Γ_σ, $\Gamma_{p\sigma}$, Γ_p, Γ_δ are positive kinetic coefficients; n_ε, n_p, n_δ are constants responsible for the velocity sensitivity of the material; F is the potential of nonequilibrium free energy; $\mathbf{p}$ is the tensor of the density of microshears, which in its physical meaning is a deformation caused by defects; $p = \sqrt{\mathbf{p} : \mathbf{p}}$; δ is the parameter of structural scaling, which in its physical meaning is the ratio of two characteristic

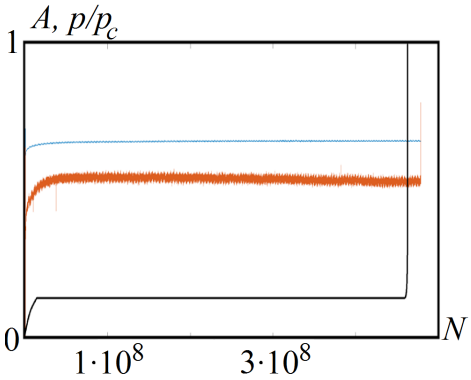

Fig. 3. (Color online) Amplitude of the first (blue line) and second (red line) harmonics in normalized units for a sample tested at 300 MPa, NS-state. The black line shows the graph of the accumulation of defects in the numerical calculation.

dimensions (distance between defects and size of defects) in a cube; c is the specific heat capacity; α is the thermal conductivity coefficient; T is the temperature; $\Delta(\cdot)$ is the Laplace operator; F_m, $c_1 - c_4$ — constants of approximation of the free energy F; T_c, m are constants of approximation of the characteristic activation energy U; **R** is the orthogonal tensor of the polar decomposition of the deformation gradient $\mathbf{F} = \mathbf{R} \cdot \mathbf{U}$, where **U** is the right symmetric positive definite distortion tensor.

To identify the parameters of the model, we used the approach proposed earlier [26].

Model parameter values for VT1-0:

SMC-state: $\Gamma_\sigma = 2.9 \cdot 10^{-9}$ $(\text{Pa} \cdot \text{s})^{-1}$, $\Gamma_{p\sigma} = 1.7 \cdot 10^{-10}$ $(\text{Pa} \cdot \text{s})^{-1}$, $\Gamma_p = 1.3 \cdot 10^{-11}$ $(\text{Pa} \cdot \text{s})^{-1}$, $\Gamma_\delta = 11.7$ $(\text{Pa} \cdot \text{s})^{-1}$, $n_\varepsilon = n_p = 0.985$, $n_\delta = 1.9$, $G = 40 \cdot 10^9$ Pa, $\delta_0 = 1.3$.

NS-state: $\Gamma_\sigma = 2.9 \cdot 10^{-9}$ $(\text{Pa} \cdot \text{s})^{-1}$, $\Gamma_{p\sigma} = 1.7 \cdot 10^{-10}$ $(\text{Pa} \cdot \text{s})^{-1}$, $\Gamma_p = 1.3 \cdot 10^{-11}$ $(\text{Pa} \cdot \text{s})^{-1}$, $\Gamma_\delta = 11.7$ $(\text{Pa} \cdot \text{s})^{-1}$, $n_\varepsilon = n_p = 0.99$, $n_\delta = 1.6$, $G = 40 \cdot 10^9$ Pa, $\delta_0 = 1.5$.

The values of the parameter δ reflect the current structural state of the material. Values less than 1 correspond to a brittle material. Values from 1 to 1.3 correspond to typical plastic materials. Values more than 1.3 correspond to nanostructured materials. The condition $\delta \le \delta_f \approx 0.4$ was used as a fracture criterion, the meaning of which is that the size of defects reaches a critical value. The simulation results are shown in Fig. 3 – 6.

We can say that the calculations and experiments are in good agreement. Experimental points that do not fall on the calculated *S-N*-curve are inconsistent for the Wöhler curve in principle, since a decrease in stress amplitude with an increase in the number of cycles should be observed (Fig. 4, 5). However, the outliers can be considered a different structural state of the material (within the framework of the NS or SMC state). "Hitting" the drop-out points can be achieved by setting the initial condition to a different value δ_0. In particular, if instead of $\delta_0 = 1.5$ set $\delta_0 = 1.8$, then it is possible to predict the "drop-out" experiment (the calculation results are shown in Fig. 3). It can be seen that the proposed model is not only capable of describing the Wöhler curve, but also qualitatively reflects the process of damage accumulation under fatigue loading.

Eqs. (4, 5, 7 – 12) are embedded in the Abaqus package using the custom VUmat procedure for 2D and 3D modeling. Direct numerical simulation of the growth of a fatigue crack and its emergence to the surface using the finite element method has been carried out. The process of laboratory specimen loading is considered in an axisymmetric formulation (the geometry is shown in Fig. 6 on the left). Direct calculation of the initiation and growth of a fatigue crack during VHCF even in an axisymmetric formulation will take a significantly long computation time. Therefore, an option is considered when the crack has already begun (the last 10^6 cycles before fracture). When the fracture criterion is reached in a specific finite element, it is given zero stiffness in the further calculation. This method of fracture modeling is an alternative to removing the corresponding element from the calculation. The results are shown in Fig. 6. In Fig. 6 shows the intensity field of the microshear density tensor referred to its characteristic value. The nonlinear dynamics of crack growth is described qualitatively: at the beginning it is slow, and at the end — an avalanche-like growth.

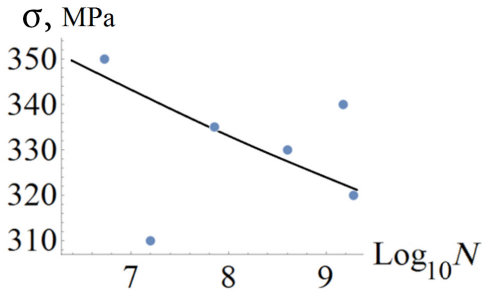

Fig. 4. Experimental (points) and calculated Wöhler curves for VT1-0 in the SMC state.

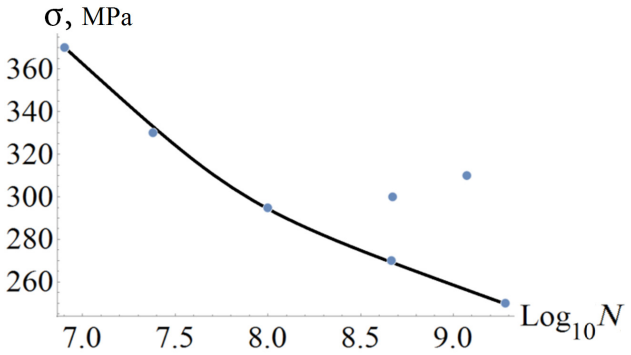

Fig. 5. Experimental (points) and calculated Wöhler curves for VT1-0 in the NS state.

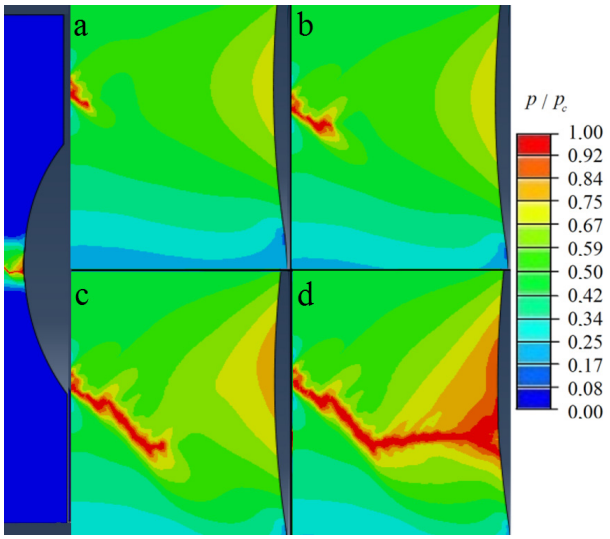

Fig. 6. (Color online) Calculation of fatigue crack growth: $5.0 \cdot 10^5$ cycles (a), $8.0 \cdot 10^5$ cycles (b), $9.5 \cdot 10^5$ cycles (c), $9.9 \cdot 10^5$ cycles (d).

4. Conclusion

An experimental study of VT1-0 titanium in various structural states has been carried out. It is shown that the endurance limit based on 10^9 cycles for the SMC state is higher than for the HC state: 320 and 250 MPa, respectively.

The proposed technique, based on the analysis of the vibration amplitude of the free end of the sample, makes it possible to track the accumulation of damage in the material in real time.

The proposed mathematical model makes it possible to adequately describe the deformation behavior and fracture of the materials under study under fatigue loading. The solution to the boundary value problem of the growth of a subsurface crack demonstrates the possibility of using the constructed model for calculating the strength and durability of real structures and separately taken critical structural elements.

Acknowledgements. This work was supported by the Russian Science Foundation, project no. 19-12-00221.

References

1. C. Bathias, P. Paris. Int. J. Fatigue. 32 (6), 894 (2010). Crossref
2. Z. Huang, D. Wagner, C. Bathias, P. C. Paris. Acta Mater. 58 (18), 6046 (2010). Crossref
3. M. A. Meyers, A. Mishra, D. J. Benson. Progress in materials science. 51 (4), 427 (2006). Crossref
4. I. A. Ovid'ko, R. Z. Valiev, Y. T. Zhu. Progress in materials science. 94, 462 (2018). Crossref
5. E. V. Naydenkin, I. V. Ratochka, I. P. Mishin, O. N. Lykova, N. V. Varlamova. Journal of Materials Science. 52 (8), 4164 (2017). Crossref
6. E. Naydenkin, G. Grabovetskaya, K. Ivanov. Materials Science Forum. 683, 69 (2011). Crossref
7. A. Vinogradov, S. Hashimoto. Materials Transactions. 42 (1), 74 (2001). Crossref
8. H. W. Höppel. Materials Science Forum. 503 – 504, 259 (2006). Crossref
9. V. F. Terent'ev, S. V. Dobatkin, S. A. Nikulin, V. I. Kopylov, D. V. Prosvirin, S. O. Rogachev, I. O. Bannykh. Russian Metallurgy. 2011, 981 (2011). Crossref
10. H. Mughrabi. Philosophical Transactions of the Royal Society A: Mathematical, Physical and Engineering Sciences. 373 (2038), 20140132 (2015). Crossref
11. T. Sakai. Jour. Solid Mech. and Mat. Eng. 3 (3), 425 (2009). Crossref
12. Y.-D. Li, L.-L. Zhang, Y.-H. Fei, X.-Y. Liu, M.-X. Li. Int. J. Fatigue. 82 (3), 402 (2016). Crossref
13. J. H. Cantrell, W. T. Yost. Int. J. Fatigue. 23 (1), 487 (2001). Crossref
14. A. Kumar, C. J. Torbet, T. M. Pollock, J. J. Wayne. Acta Mater. 58 (6), 2143 (2010). Crossref
15. A. Kumar, R. R. Adharapurapu, J. W. Jones, T. M. Pollock. Scr. Mater. 64 (1), 65 (2011). Crossref
16. A. Demčenko, R. Akkerman, P. B. Nagy, R. Loendersloot. NDT & E International. 49, 34 (2012). Crossref
17. Y. Yang, C. T. Ng, A. Kotousov, H. Sohn, H. J. Lim. Mechanical Systems and Signal Processing. 99 (1), 760 (2018). Crossref
18. J. Kober, Z. Prevorovsky. NDT & E International. 61 (1), 10 (2014). Crossref
19. Z. Su, C. Zhou, M. Hong, L. Cheng, Q. Wang, X. Qing. Mechanical Systems and Signal Processing. 45 (1), 225 (2014). Crossref
20. P. Liu, H. Sohn, T. Kundu, S. Yang. NDT & E International. 66, 106 (2014). Crossref
21. Yu. R. Kolobov. Nanotechnologies in Russia. 4 (11-12), 758 (2009). Crossref
22. S. S. Manokhin, A. Y. Tokmacheva-Kolobova, Y. Y. Karlagina, V. I. Betekhtin, A. G. Kadomtsev, M. V. Narykova, Y. R. Kolobov. Journal of Surface Investigation. 15 (1), 59 (2021). Crossref
23. M. V. Narykova, A. G. Kadomtsev, V. I. Betekhtin, Yu. R. Kolobov, S. S. Manohin, A. Yu. Tokmacheva. Journal of Physics: Conference Series. 1697 (1), 012113 (2020). Crossref
24. B. K. Kardashev, M. V. Narykova, V. I. Betekhtin, A. G. Kadomtsev. Physical Mesomechanics. 23 (3), 193 (2020). Crossref
25. O. B. Naimark. Physical mesomechanics. 6 (4), 39 (2003).
26. D. A. Bilalov, V. A. Oborin, O. B. Naimark, M. V. Narykova, A. G. Kadomtsev, V. I. Betekhtin. Technical Physics Letters. 46 (4), 397 (2020). Crossref